



Efficient ionic liquid-based platform for multi-enzymatic conversion of carbon dioxide to methanol

Zhang, Zhibo; Muschiol, Jan; Huang, Yuhong; Sigurdardóttir, Sigyn Björk; von Solms, Nicolas; Daugaard, Anders E.; Wei, Jiang; Luo, Jianquan; Xu, Bao-Hua; Zhang, Suojia

Total number of authors:
11

Published in:
Green Chemistry

Link to article, DOI:
[10.1039/c8gc02230e](https://doi.org/10.1039/c8gc02230e)

Publication date:
2018

Document Version
Peer reviewed version

[Link back to DTU Orbit](#)

Citation (APA):

Zhang, Z., Muschiol, J., Huang, Y., Sigurdardóttir, S. B., von Solms, N., Daugaard, A. E., Wei, J., Luo, J., Xu, B.-H., Zhang, S., & Pinelo, M. (2018). Efficient ionic liquid-based platform for multi-enzymatic conversion of carbon dioxide to methanol. *Green Chemistry*, 20(18), 4339-4348. <https://doi.org/10.1039/c8gc02230e>

General rights

Copyright and moral rights for the publications made accessible in the public portal are retained by the authors and/or other copyright owners and it is a condition of accessing publications that users recognise and abide by the legal requirements associated with these rights.

- Users may download and print one copy of any publication from the public portal for the purpose of private study or research.
- You may not further distribute the material or use it for any profit-making activity or commercial gain
- You may freely distribute the URL identifying the publication in the public portal

If you believe that this document breaches copyright please contact us providing details, and we will remove access to the work immediately and investigate your claim.

Zhang, Z., Muschiol, J., Huang, Y., Sigurdardóttir, S. B., von Solms, N., Daugaard, A. E., ...
Pinelo, M. (2018). Efficient ionic liquid-based platform for multi-enzymatic conversion of
carbon dioxide to methanol. *Green Chemistry*, 20(18), 4339-4348.
<https://doi.org/10.1039/c8gc02230e>

Efficient Ionic Liquid-based platform for Multi-Enzymatic Conversion of Carbon Dioxide to Methanol

Zhibo Zhang,^{a,b} Jan Muschiol,^a Yuhong Huang,^a Sigyn Björk Sigurdardóttir,^a
Nicolas von Solms,^a Anders E. Daugaard,^a Jiang Wei,^a Jianquan Luo,^c
Bao-Hua Xu,^b Suojian Zhang^{*b} and Manuel Pinelo^{*a}

Low yields commonly obtained during enzymatic conversion of CO₂ to methanol are attributed to low CO₂ solubility in water. In this study, four selected ionic liquids with high CO₂ solubility were separately added to the multi-enzyme reaction mixture and the yields compared to pure aqueous system (control). In an aqueous 20% [CH][Glu] system, yield increased app. 3.5-fold compared to the control (app. 5-fold if NADH regeneration was incorporated). Molecular dynamics simulation revealed that CO₂ remains for longer in a productive conformation in the enzyme in the presence of [CH][Glu], which explains the marked increase of yield that was also confirmed by isothermal titration calorimetry - lower energy (ΔG) binding of CO₂ to FDH-. The results suggest that the accessibility of CO₂ to the enzyme active site depends on the absence/presence and nature of the ionic liquid, and that the enzyme conformation determines CO₂ retention and hence final conversion.

^aDepartment of Chemical and Biochemical Engineering, Building 229, Technical University of Denmark, DK-2800 Kgs. Lyngby, Denmark. E-mail: mp@kt.dtu.dk
^bBeijing Key Laboratory of Ionic Liquids Clean Process, Key Laboratory of Green Process and Engineering, State Key Laboratory of Multiphase Complex Systems, Institute of Process Engineering, Chinese Academy of Sciences, Beijing 100190, P. R. China. E-mail: sjzhang@ipe.ac.cn
^cState Key Laboratory of Biochemical Engineering, Institute of Process Engineering, Chinese Academy of Sciences, Beijing 100190, PR China

Introduction

One of the greatest environmental challenges we face today are the large emissions of carbon dioxide (CO₂) into the atmosphere each year, which contribute to global warming, ocean acidification, melting of icebergs and the energy crisis.^{1,2} Ideally, CO₂ ought to be converted to useful chemical and fuels (e.g. methanol) for renewable energy utilization and simultaneously alleviation of the problem of CO₂ emissions. Therefore extensive efforts have been made to bring about catalytic hydrogenation of CO₂ via chemistry, electrochemistry, photochemistry and enzymatic conversions.^{3,4,5,6} Due to the inherent thermodynamic stability and low reactivity of CO₂, production of methanol by enzymatic conversion has significant advantages over conventional techniques owing to the high selectivity, high efficiency, mild experimental conditions, and environmental friendliness of enzymatic catalysis.⁶

Inspired by the biological metabolic pathway, sequential reduction of CO₂ to formic acid, formaldehyde and methanol can be achieved by using formate dehydrogenase (FDH), formaldehyde dehydrogenase (FaldDH), and alcohol dehydrogenase (ADH), respectively.^{6,7,8} However, the yield of methanol achieved in this type of system is only 43.8%.⁷ The low conversion was partly explained by the fact that the reaction rate of the first reaction in the sequence (CO₂→formic acid), catalysed by FDH, is much slower than its reverse reaction (formic acid→CO₂).

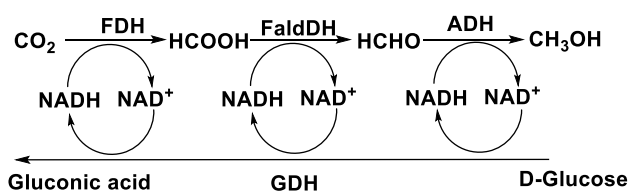
Indeed, Rusching et al. reported that formic acid oxidation was 30 times faster than CO₂ reduction catalyzed by FDH.⁹ Thus the CO₂→formic acid step is likely to be a bottleneck in the reduction of CO₂ to methanol. In this regard, we envisioned that a higher yield of product, either formaldehyde or methanol, could be reached by increasing the concentration of substrate (CO₂) in the solution, which may drive the transformation of CO₂ to formic acid forward. In addition, it could also be helpful to further promote the reaction rate by incorporating a membrane to the system so that products would be immediately separated from reaction and thus switch the equilibrium towards the formic acid.

Ionic liquids (ILs) have great capacity to capture CO₂ *via* electrostatic forces, van der Waals forces, hydrogen bonds and other physical effects.¹⁰ Amine functionalized cation-tethered ILs have been used for CO₂ capture, in which 0.5 mol CO₂ per mol of IL could be absorbed through a carbamate mechanism.¹¹ Amino acid ILs could capture almost 1 mol CO₂ per mol of IL by forming carbamic acid rather than carbamate.¹² Furthermore, the high potential of CO₂ electronic reduction could be lowered by ILs to achieve a lower energy barrier.^{13, 14} To date, ILs have been used in various enzymatic reactions, e.g. with cellulases and ADH.^{15, 16, 17, 18} Recently, several biocompatible and environmentally friendly ILs have been identified which are composed of naturally-derived materials such as sugars, amino acids, and choline.¹⁹ Several proteins have been successfully dissolved in choline dihydrogenphosphate [CH][DHP] without denaturation.²⁰ 70% of the initial redox activity of Cytochrome C remained more than one year after dissolving in a mixture of [CH][DHP] and water.²¹ Amino acid-based ILs as benign media have been also reported in biomedical applications.^{22, 23} ILs could thus be promising substitutes of traditional buffers for conducting selected enzymatic reactions.

For in-situ removal of products (methanol and NAD⁺) and recycling of enzymes, a separation system platform is additionally required. Recently, inspired by membrane fouling mechanisms, we proposed a simple approach to immobilize enzymes in membranes using “reverse filtration” of the enzyme solution.⁸ In this system, enzyme immobilization was achieved by hydrogen bonding, entrapment and hydrophobic or electrostatic adsorption.²⁴ The activity of the immobilized enzymes could be maintained to approximately that of the free enzymes due to the mild and fast immobilization procedure. High enzyme loading could also be maintained and the contact time substrate-enzyme could be controlled by changing pressure. However, to produce one mole of methanol in such a cascade reaction, three moles of reduced nicotinamide adenine dinucleotide (NADH) are stoichiometrically consumed, as the cofactor (NADH) acts as a hydrogen and electron donor at each step of the reduction reaction.²⁵ Converting the oxidized form of the cofactor (NAD⁺) to NADH is essential for reducing cost and enhancing methanol production. Normally, NADH regeneration is accomplished by chemical, photochemical, and electrochemical methods, but such regeneration can be also attained by adding another enzyme system which requires NAD⁺ to proceed (**Scheme 1**).²⁶

In this study, biocompatible ILs composed of choline and amino acids (i.e. [CH][Glu], [CH][Pro], [CH][Gly], and [CH][His]) were designed and synthesized in order to increase CO₂ solubility and stabilize FDH. These ILs were incorporated in a membrane reactor system which enabled in situ removal of products from the reaction, as illustrated in **Figure 1**. Four kinds of ILs as co-solvent were evaluated in the biocatalytic membrane reactor by passing a mixture of CO₂, IL and cofactor through the enzyme-loaded membrane. To our knowledge, this is the first report of multi-enzymatic conversion of CO₂ to methanol in ILs with NADH regeneration. This integration of ILs and biocatalytic membrane provides a promising avenue for a practical CO₂-based sustainable chemistry.

Results and Discussion



Scheme 1. Multi-enzyme system for methanol synthesis from CO₂ with in situ regeneration of NADH.

Fabrication of biocatalytic membrane. The immobilization was performed in a membrane assembled in a so-called sandwich mode (polypropylene layer – skin layer – polypropylene support) so that the membrane support layer was positioned to face the feed, while underneath the skin layer an extra polypropylene support was placed to act as a cushion to alleviate membrane compression and peeling of the skin layer (**Figure 1**). Based on the “fouling-induced immobilization” method, the three enzymes (i.e. FDH, FaldDH and ADH) were simultaneously immobilized in the membrane. During enzyme loading in the membrane, the permeate volume over time was collected, as presented in **Figure S1**. The mechanism of membrane fouling induced by the enzyme solution filtration was categorized into four fouling models which are presented in **Table S1** and identified as standard, intermediate, complete blocking, and cake layer models.^{27, 28} The cake layer model, showing a high value correlation coefficient, was found to best describe the loading mechanism. In the initial stage of the filtration process, only the cake layer model fitted the experimental data, which indicated that most enzymes are deposited on the skin layer of the membrane. As filtration time increased, the experimental data also correlated well with other models because the fouling layer created by the enzymes acts as an additional membrane.⁸ The morphology of the enzyme-immobilized membrane was characterized by SEM, and is shown in **Figure 2**. The figure shows the skin layer, which is made up of regenerated cellulose (**Figure 2a**), and some enzyme aggregates adsorbed on the surface of the polypropylene support fibres (**Figure 2b,c**). From the mathematical modelling and characterization by SEM, the fouling-induced enzyme immobilization was found to involve at least two mechanisms: entrapment and adsorption. In **Figure 2c** it can be seen that some enzymes were bound to the support fibres by hydrophobic adsorption. Based on mass balance calculations by Bradford assay, 2.66 mg of protein was immobilized in the membrane, which corresponds to enzyme loading efficiency of 76%. Accordingly, the permeability dropped to 3.04 L m⁻² h⁻¹ bar⁻¹ after enzyme loading, which is around 10 times lower than that of virgin membrane (330 ± 6 L m⁻² h⁻¹ bar⁻¹).

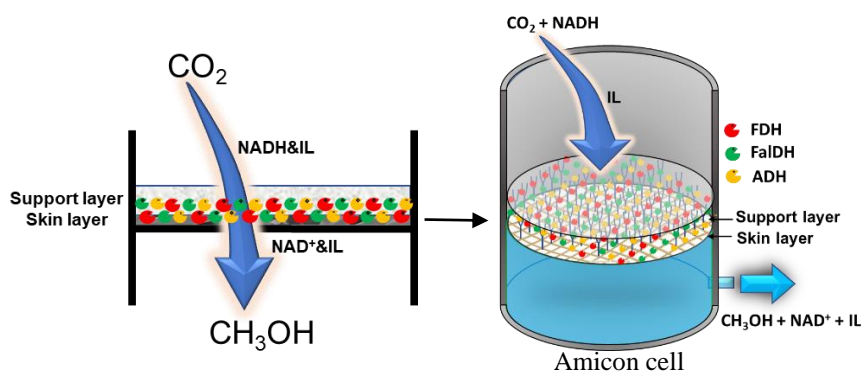


Figure 1. The immobilization strategy of enzymes in membrane for multi-enzymatic cascade reaction.

The synthesis of methanol from CO₂ catalyzed by the three-enzyme cascade reaction in Tris-HCl buffer was performed with the membrane loaded with enzymes. According to the reaction route, three moles of NADH are stoichiometrically consumed to produce one mole of methanol in the cascade reaction. Therefore the methanol yield (Y_{methanol}) based on NADH may be calculated using the following equation.

$$Y_{\text{methanol}} (\%) = \frac{C_{\text{methanol}} * 3}{C_{\text{NADH,initial}}} * 100$$

Where C_{methanol} is the methanol concentration (mM), and $C_{\text{NADH,initial}}$ is the initial NADH concentration (mM).

After 30 min reaction, a methanol yield of 24.5% was obtained for the immobilized system, whilst practically the same yield (23.5%) was obtained for an equivalent free enzyme system (using the same amount of enzymes in free form) (**Figure 3a**). The similar yield obtained confirmed that no enzyme activity was sacrificed during immobilization. The low yield of methanol obtained was explained by the kinetics of the reaction, as reported by Luo et al.⁸ As explained above, the reaction rate of the forward reaction ($\text{CO}_2 \rightarrow \text{formic acid}$) is much lower than that of the reverse reaction ($\text{formic acid} \rightarrow \text{CO}_2$). For the second enzyme, FaldDH, the reaction ($\text{formic acid} \rightarrow \text{formaldehyde}$) was also found to be less efficient than the reverse reaction ($\text{formaldehyde} \rightarrow \text{formic acid}$). However, for the third enzyme, ADH, the forward reaction ($\text{formaldehyde} \rightarrow \text{methanol}$) was much more efficient than the reverse reaction ($\text{methanol} \rightarrow \text{formaldehyde}$).⁸ Additionally, Luo et al. suggested that in order to be activated, the second reaction required a threshold concentration of formic acid. Therefore the first reaction from CO_2 to formic acid probably plays a decisive role in this cascade reaction.



Figure 2. (a) SEM images of (a) skin layer (regenerated cellulose) Overview of skin layer (regenerated cellulose); (b) support layer (polypropylene nonwoven fibers); (c) View of support layer after enzyme immobilization.

Muti-enzymatic reaction in the ILs with co-immobilization of enzymes. The four selected ILs have a high capacity to absorb CO_2 , where one mole of IL can chemically absorb half a mole of CO_2 .²⁹ The adsorption of half a mole of CO_2 by each mole of IL was proposed by Han et al, and similar mechanisms of CO_2 adsorption by ILs were also reported by other authors.^{11, 29, 30} Han et al also demonstrated that $[\text{CH}][\text{AA}]$ can be repeatedly recycled for CO_2 adsorption, owing to CO_2 can be desorbed from IL by bubbling N_2 . Therefore, the process of CO_2 adsorption is reversible, and ILs can provide FDH with a proper CO_2 concentration with a slow-releasing system, as required by FDH. As illustrated in **Figure 3a** (red points), the measured molar ratio of CO_2 to the ILs could slightly exceed 0.5. The slightly excess of CO_2 :IL molar ratio suggests that physical adsorption could also contribute to the uptake of CO_2 . Based on the CO_2 solubility in the pure ILs, the CO_2 concentration in the four kinds of 20% ILs was calculated to be in the range from 467 to 714 mM, which is far higher than the CO_2 solubility in water (33 mM).³¹ Furthermore, the CO_2 adsorption rate in an aqueous IL solution is faster than in the pure IL. Indeed, CO_2 adsorption equilibrium is reached after 20 minutes in aqueous 5 wt% $[\text{CH}][\text{AA}]$, whilst the saturation of CO_2 in pure $[\text{CH}][\text{AA}]$ will take at least 4 h.^{29, 32} Therefore aqueous ILs can be as such an ideal medium for enzymatic reactions.

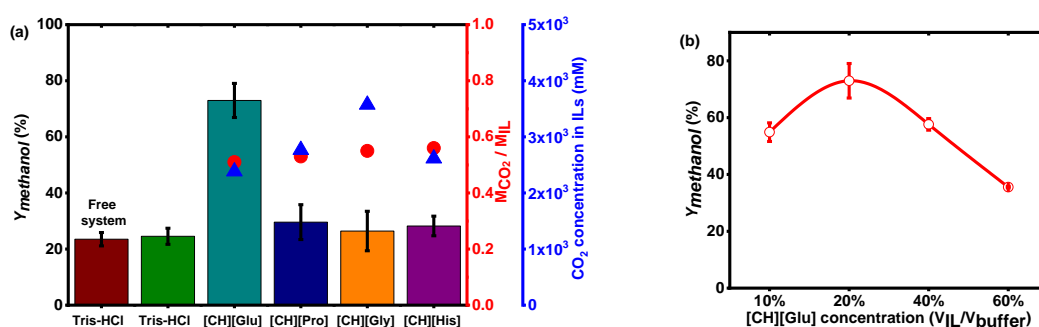


Figure 3. (a) Yield of methanol in Tris-HCl (pH=7.0) and in four kinds of 20% ILs (left); solubility of CO₂ in the absolute ILs with molar ratio of CO₂ to the IL (M_{CO_2}/M_{IL}) (left, red circle); CO₂ concentration in ILs (left, blue triangle). All the enzymatic reactions were conducted in the membrane except “Free system”. (b) Methanol production at different concentrations of [CH][Glu]. An enzymatic membrane reactor equipped with a 10 kDa regenerated cellulose membrane (skin layer facing feed) was used. Recycling of immobilized enzymes was conducted using fresh NADH solution in Tris-HCl buffer and containing 20% [CH][Glu] buffer (NADH = 5 mM).

CO₂ reduction to methanol with the enzyme-loaded membrane (i.e. FDH, FaldDH, and ADH) was performed in the presence of 20% ILs ($V_{IL}/V_{buffer} = 20\%$) (**Figure 3a**). The maximum methanol yield was achieved using [CH][Glu] and was ~3.5 times higher than the results of multi-enzymatic reactions in Tris-HCl buffer. The same reaction was similarly examined for the other three ILs, but conversion of CO₂ was not significantly improved compared to the reactions in Tris-HCl buffer. In the past, Liu et al. increased the pressure during operation as an additional strategy to achieve high CO₂ concentration in solution. They found that the reaction rate increased from $(1.20 \pm 0.09) \times 10^{-3}$ to $(2.17 \pm 0.07) \times 10^{-3}$ $\mu\text{mol}/\text{min}$ when CO₂ pressure was increased from 0.2 MPa to 0.5 MPa, but almost no change was detected when pressure was further increased to 1.0 MPa.³³ The stable yield detected when pressure was increased above 0.5 MPa was attributed to the fact that NADH concentration probably became the limiting factor. In our case, methanol yield could be improved almost three fold by increasing the CO₂ concentration 15 times in the [CH][Glu] system compared to reactions in Tris-HCl buffer.

To further improve the efficiency of CO₂ conversion, the [CH][Glu] concentration was studied over the range 10% to 60% [CH][Glu]. The yield of methanol was clearly increased with increasing [CH][Glu] from 10% to 20%. CO₂ captured in the solution was noticeably increased by increasing [CH][Glu] concentration, thus shifting the reaction equilibrium towards the production of methanol. However, the yield of methanol declined with further increase of the [CH][Glu] concentration from 20% to 60%. Although more CO₂ was captured by increasing the IL concentration, conformational changes of the peptide chains of the enzymes could have contributed to the decrease in the activity. Indeed, increasing organic salts concentration has been reported to affect the electrostatic balance in the proteins, with a direct effect on activity.³⁴ Furthermore, stability, crystallisation behaviour and aggregation behaviour of proteins have been reported to change dramatically with increasing concentration of ILs in aqueous media.^{35, 36, 37} Previous studies have also confirmed the difficulty of homogeneously dissolving the proteins in pure ILs without denaturation.^{38, 39} Therefore water-based solvents with small amounts of salts (water-rich IL mixtures) are believed to be the best media for proteins.³⁴ This balance between CO₂ solubility and protein denaturation can tentatively explain why 20% [CH][Glu] as co-solvent provided the highest yield.

pH effect on enzyme activity. Liu et al. reported that the optimal pH for reduction of CO₂ to formic acid by FDH was 6.0⁴⁰. However, neutral conditions (pH 7.0) resulted in the highest formaldehyde production from conversion of formic acid to formaldehyde catalysed by FaldDH. ADH, the third enzyme in the sequence, was reported to have an optimal activity at pH 8.1 by Shrabon.⁴¹ In our case, the optimum pH value when the reaction took place in buffer (without ionic liquids) was 6.5, which is similar to the optimum pH of FDH (**Figure 4a**); this result may suggest that the first reaction (CO₂→Formic acid) plays a decisive role in the performance of the whole reaction.

The relative activity was also found to significantly decrease when the pH value of the buffer was either below 6.5 or above 7.5, which suggests reduced enzyme activity under both acid and alkali conditions. Previous studies suggested that the activity and structure of the enzymes might be affected by strongly acidic or alkaline media.⁴² Our results showed that the pH of the 20% [CH][Glu] mixture (pH 6.85) was lower than the pH of the other ILs screened, which could also have influenced the higher conversion of the former compared to the ILs evaluated. Unfortunately, these ILs were synthesized by acid-base neutralization of choline and amino acids. Therefore lowering the pH of the other ILs was not possible because to do so would have resulted in decomposition and amino acid precipitation from the solution; thus no direct comparison among the four ILs at the same pH could be performed.

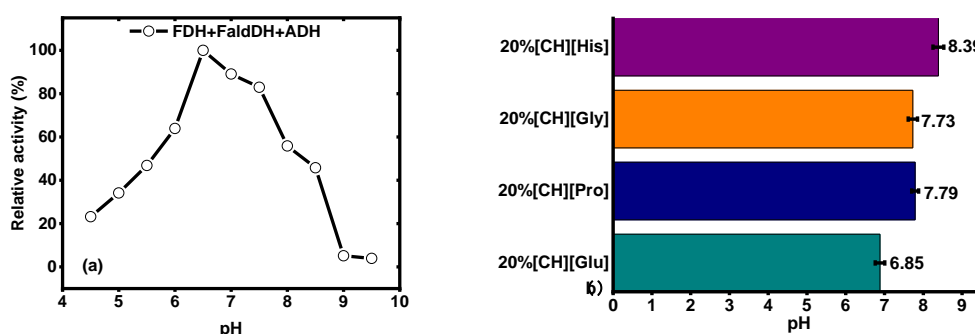


Figure 4. (a) Activity of the three enzymes at different pH from 4.5 to 9.5; (b) pH values in different kinds of 20% ILs (V_{IL}/V_{Buffer}) after 30 min bubbling with CO_2 .

Recycle of the biocatalytic membrane. To evaluate the recyclability of the biocatalytic membrane, FDH, FaldDH and ADH were co-immobilized in the 10 kDa regenerated cellulose membrane and fresh substrate was fed to the reactor after each of the six 30-minutes reaction cycles. The yield of methanol in the Tris-HCl buffer was maintained at 20% - 40% for six runs (Figure 5), which confirmed that enzyme leakage was low and that enzyme activity was not lost during immobilization. In the presence of [CH][Glu], the yield of methanol increased and was between 60% to 75% during the six runs. A slight decrease in the yield (albeit not significant) was observed after the second run, but no further decrease was observed during the remaining four runs

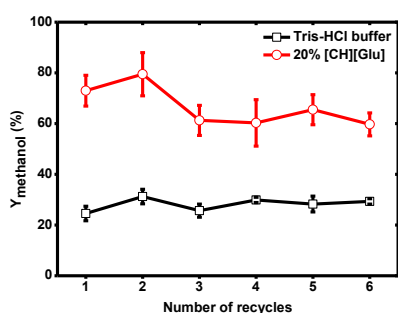


Figure 5. Stability of biocatalytic membrane in Tris-HCl buffer and 20% [CH][Glu].

Cofactor (NADH) regeneration with glucose dehydrogenase. NADH acts as a terminal electron donor and hydrogen donor in the cascade enzymatic reaction and is consumed stoichiometrically at each step. As a result, three molar equivalents of NADH are consumed to transform one molar equivalent of CO_2 in methanol. Efficient regeneration of NADH is crucial for such a cascade enzymatic reaction since the cost of NADH is very high and in-situ generated NAD^+ will in turn inhibit the reduction of CO_2 and promote the reverse oxidative reaction. In the current study, glucose dehydrogenase (GDH) was used for NADH regeneration and the enzymatic reaction was

coupled to the main cascade enzymatic reaction. Therefore GDH was immobilized together with the three enzymes (FDH, FaldDH, ADH) in the 10 kDa regenerated cellulose membrane. D-glucose (50 mM) as the GDH substrate was mixed with NADH solution (4 mL) containing 20% [CH][Glu], which was pre-bubbled with CO₂ for 30 minutes. As seen in **Figure 6**, the yield of methanol increased from 73% to 102% after 30 to 120 min reaction and then reached equilibrium after 120 min. The result indicates that NADH was efficiently regenerated with high activity of GDH. A number of researchers have also reported that the yield of methanol increased with increasing NADH concentration.^{43, 44, 45, 46} Total turnover number (TTN) of up to 10000 has been obtained by using GDH for the regeneration of NAD⁺, as reported by Obon.⁴⁷ The reduction rate from NAD⁺ to NADH catalysed by GDH is faster than the oxidation of NADH to NAD⁺ by ADH, as reported by Fauziah et al.²⁶ The reaction rate for the reaction from NAD⁺ to NADH catalysed by GDH was 6.3 $\mu\text{mol/mg}\cdot\text{min}$, while the reaction rate for the reaction from NADH to NAD⁺ catalysed by ADH was 4.7 $\mu\text{mol/mg}\cdot\text{min}$. Furthermore, converting NADH to NAD⁺ catalysed by ADH was much more efficient than with the other two enzymes (FDH and FaldDH).⁸ The reaction rate for the cascade reaction is limited by the slowest reaction. Therefore the reaction rate for converting NAD⁺ to NADH is far higher than the oxidation of NADH by the three enzymes. Lastly, after two hours there was no further improvement in yield of methanol. Probably, due to product inhibition by high methanol concentration in the solution, the reversible enzymatic reaction would progress any further.

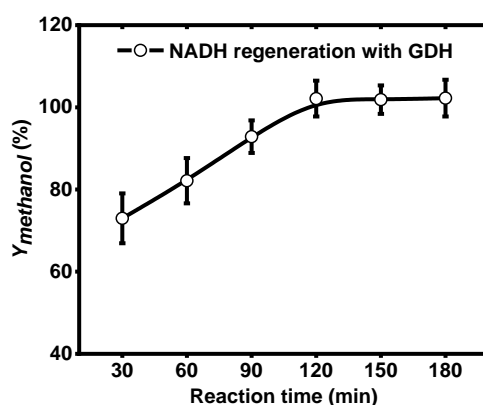


Figure 6. Methanol production as a function of reaction time with coupled GDH for cofactor regeneration

Molecular Simulation. Molecular dynamics simulations on FDH with different solvents (i.e. water, 20%[CH][Gly], 20%[CH][Glu], 20%[CH][His] and 20% [CH][Pro]) were performed in order to evaluate the effect of the aqueous IL on the enzyme. As depicted in **Figure 7a**, all simulations using aqueous ILs showed a similar trend with respect to the root mean square deviation (RMSD) value of the C α backbone over the MD simulation time, with the exception of 20% [CH][Glu] which approached a lower maximum value. The average RMSD values for the simulation in water and using the aqueous ILs (except [CH][Glu]) ranged from 1.7 to 1.9 Å (**Figure S2**). In contrast, the average RMSD values for the 20% [CH][Glu] simulation of 1.3 Å were markedly lower compared to the other solvents (**Figure S2**). These results might also indicate a stabilizing effect of the aqueous 20% [CH][Glu] on protein structural integrity and therefore be another explanation for the good performance of the 20% [CH][Glu] as solvent for the reaction system.

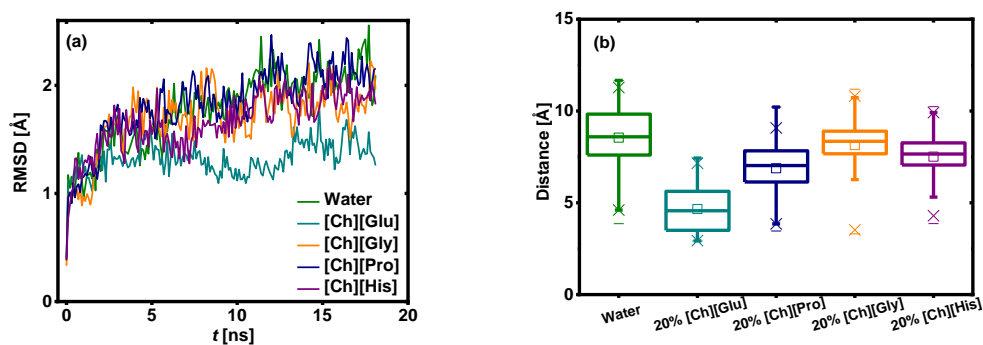


Figure 7. (a) RMSD time course during the molecular dynamics simulations using H₂O (black line), 20% [Ch][Gly] (blue line), 20% [Ch][Glu] (red line), 20% [Ch][His] (green line) and 20% [Ch][Pro] (pink line) in water as solvents. (b) Distance of the Tyr73 OH-group and Phe 285 Cζ over the MD simulation time.

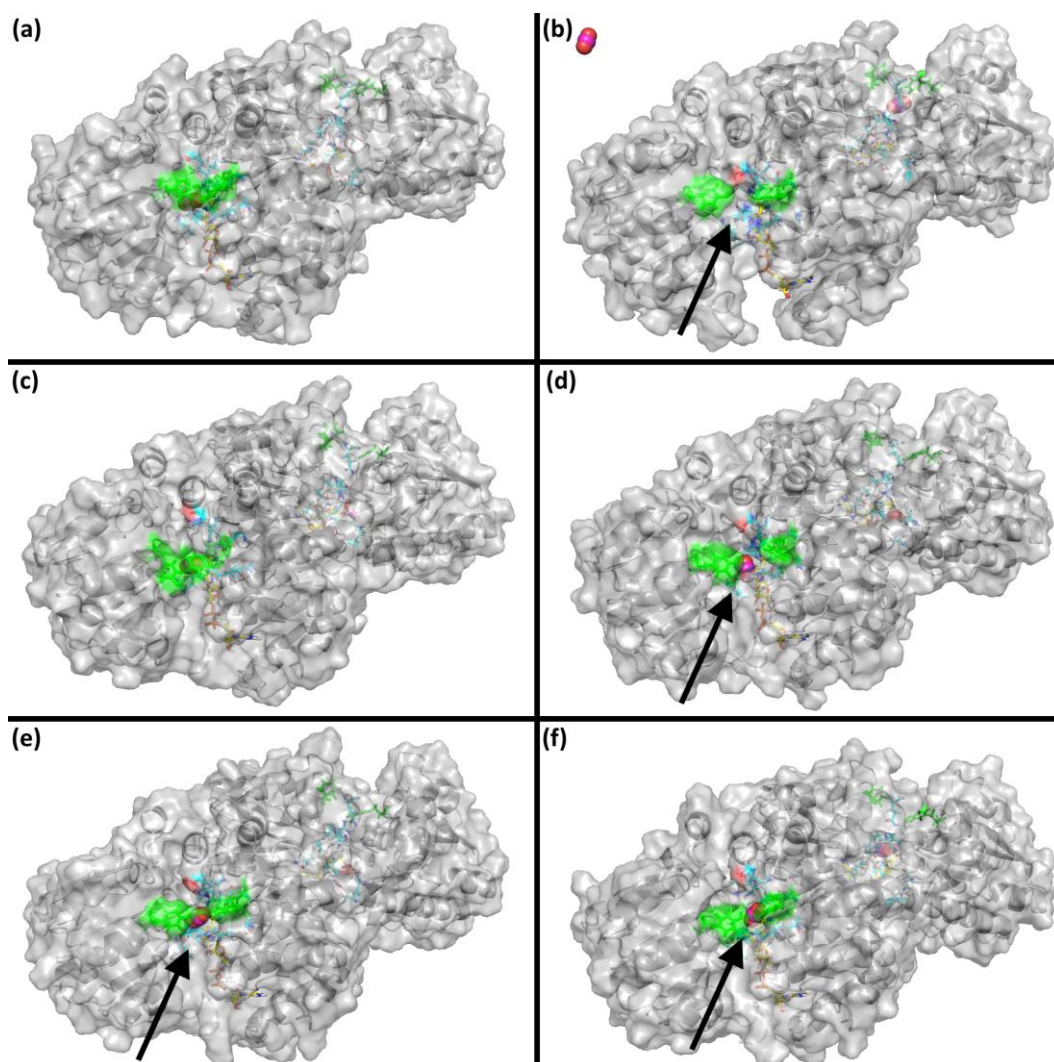


Figure 8. Surface representation of formate dehydrogenase (PDB 5DN9) at the beginning (A) and end (B-F) of MD simulation in different solvent systems: H₂O (B), 20% [Ch][Glu] (C), 20% [Ch][Gly] (D), 20% [Ch][His] (E), 20% [Ch][Pro] (F). For clarity the bulk solvent is not shown. The NADH cofactor is shown as yellow sticks, the catalytically important Arg is shown as cyan sticks, Tyr73 and Phe285 are highlighted as green ticks and green surface, CO₂ is shown as cyan spheres. The solvent accessible active sites are highlighted by a black arrow.

Closer inspection of the MD simulations revealed that in all solvent systems (except 20% [CH][Glu]) the active site, which binds the CO₂ molecule, quickly became solvent accessible (**Figure 8, Movies S1-5**). This was especially pronounced in the simulation with water as solvent where one of the CO₂ molecules has left the active site after 12.5 ns (**Figure 8b, Movie S1**). As a measure of this surface opening, the distance of the amino acid side chain OH-group of Tyr73 and the C ζ of the side-chain of Phe285 was recorded over the simulation time. The 20% [CH][Glu] exhibited significantly different behaviour compared to the other solvent systems and had a mean distance of 4.7 Å while that of the other solvent systems ranged from 6.9 – 8.5 Å (**Figure 7b**). Furthermore, detailed analysis of distance between residues and ligands involved in formation of the enzyme transition state (TS, **Figure 9A**), as reported by Castillo, et al.⁴⁸, revealed clearly that formation of the TS would be favoured far more in the 20% [CH][Glu] system than in all the other systems (**Table S4**). This effect was also reflected in the root mean square fluctuation (RMSF) values of the residues involved in positioning the CO₂ molecule inside the active site (**Figure 9B**). The amino acid side chains of Asn119, Arg258 and His311 in particular showed a significantly lower fluctuation over the MD simulation time in 20% [CH][Glu] compared to the other solvent systems. As explanation for the high yield of methanol in 20% [CH][Glu] we hypothesize that the increased rigidity of the FDH on the one hand also increases protein stability itself and on the other hand leads to an increased residence time of CO₂ in the active site in a more TS-like conformation than in the other studied solvent systems. This prolonged TS-like residence time of CO₂ in the active site increases the probability of a productive positioning of the reactants for the formation of formic acid, which thus could result in a shift of the reaction equilibrium towards the less favoured reduction of CO₂ to formic acid.

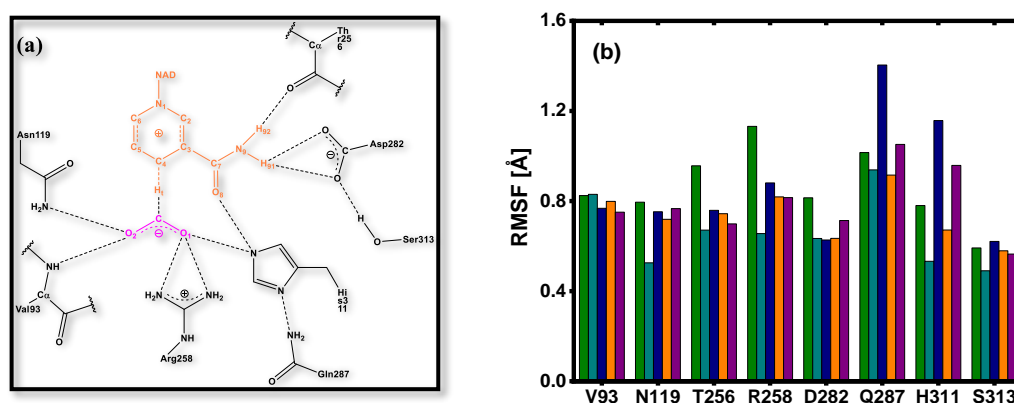


Figure 9. (A) Transition state of the FDH catalyzed reaction as proposed by Castillo et al. The NADH cofactor is highlighted in orange and the substrate CO₂ in pink. (B) RMSF values for the amino acid residues involved in substrate and co-factor binding as well as TS formation over MD simulation time for the different solvent systems: H₂O (olive bars), 20% [CH][Glu] (Cyan bars), 20% [CH][Pro] (Blue bars), 20% [CH][Gly] (Orange bars), 20% [CH][Pro] (Purple bars).

For further validation of the MD simulation, isothermal titration calorimetry (ITC) was carried out to elucidate the interaction of FDH with CO₂ in the different solvents (i.e. water and 20% [CH][Glu]). Adsorption heat due to interaction between FDH with CO₂ in water and [CH][Glu] was fitted by Nano-Analyze software (TA Instruments) using an independent model to obtain the Gibbs free energy (ΔG). As shown in **Table S1**, the ΔG value of CO₂ interactions with FDH in water was - 17.12 kJ mol⁻¹, which is higher than that of CO₂ and FDH interaction in the presence of [CH][Glu] (-18.75 kJ mol⁻¹). This indicates the binding of CO₂ due to lower enzyme flexibility in 20% [CH][Glu].

Conclusion

A straightforward enzyme loading approach inspired by membrane fouling mechanisms provided a novel platform for conducting a sequential enzyme reaction in the presence of ILs. The biocatalytic system had a promising capacity for enzyme loading and showed high stability after several experimental cycles. Previous studies have shown that the first reaction of the sequence, $\text{CO}_2 \rightarrow$ formic acid, plays a decisive role in conversion of CO_2 to methanol and represents the “bottleneck” that determines the progress of the whole reaction. A strategy to enhance the conversion of this reaction step was attempted by increasing the concentration of CO_2 in the reaction system through adding ionic liquids as a co-solvent. The system that offered the best conversion results was an aqueous mixture 20% [CH][Glu] in which CO_2 concentration was around 15 times higher than in Tris-HCl buffer as the control.

Though CO_2 concentration achieved was similar in the other ionic liquids selected, the reaction yield significantly increased only when [CH][Glu] was used. The reason for this difference was further investigated. We found that pH might play a significant role in the reaction, because slightly acidic pH seems to be favour the conversion. The most convincing explanation, however, was provided by molecular simulation dynamics. While CO_2 easily diffuses out of the active site in the other ILs tested, and especially in water, the conformation of FDH in the presence of [CH][Glu] is such that CO_2 stays for a longer time in the vicinity of the active site of the enzyme. Such longer retention times may therefore result in higher conversion of CO_2 .

Further systematic research on this topic must provide more specific information about the mechanisms and specific functional groups of ionic liquids, which are responsible for the kinds of conformational enzyme changes that can support higher conversions.

Methods

Materials. Glycine (Gly), L-proline (Pro), L-histidine (His), L-glutamic acid (Glu), Choline hydroxide (aqueous solution 46 wt%), were purchased from Sigma Aldrich (St. Louis, MO, USA). Methanol and acetonitrile were analytical grade and used without any further purification. Double-distilled water was used in all experiments. Formate dehydrogenase (EC 1.2.1.2, homo-dimer, 76 kDa) from *Candida boidinii* (FDH), formaldehyde dehydrogenase (EC 1.2.1.46, homo-dimer, 150 kDa) from *Pseudomonas* sp. (FaldDH), alcohol dehydrogenase (EC 1.1.1.1, homo-tetramer, 141 kDa) from *Saccharomyces cerevisiae* (ADH), and glucose dehydrogenase (EC 1.1.1.118, homo-hexamer, 300 kDa) from *Pseudomonas* sp. (GDH) were purchased from Sigma-Aldrich (St. Louis, MO, USA). These commercial powders or liquids are not pure enzymes and the protein content was determined by Bradford protein assay. β -Nicotinamide adenine dinucleotide reduced form (NADH, >97 wt%), β -nicotinamide adenine dinucleotide hydrate (NAD^+), Trizma base, hydrochloric acid (37%) D-glucose, and methanol ($\geq 99.9\%$) were purchased from Sigma Aldrich (St. Louis, MO, USA). All the enzyme and substrate solutions were prepared using 0.1 M Tris-HCl buffer (pH = 7.0) unless otherwise stated. CO_2 gas (>99.5%) in a cylinder was purchased from AGA A/S (Denmark). Commercial UF membranes (PLGC, Millipore) used in this work have a regenerated cellulose skin layer on a polypropylene support, and their molecular weight cut-off is 10 kDa.

Synthesis of [Ch][AA] ILs. ILs were prepared and purified according to the literature.⁴⁹ [Ch][OH] aqueous solution (about 4 M) was added dropwise under cooling to an amino acid aqueous solution or suspension (0.06 mol) to obtain a slight excess (about 10 mol%) of amino acid. The mixture was stirred at about 3 °C overnight in the

dark. Water was then removed under reduced pressure at 50 °C using a rotavapor. Acetonitrile/methanol (9 : 1, v/v) was then added under vigorous stirring to precipitate the excess of amino acid. The mixture was left stirring overnight and the excess of amino acid was then filtered off. The filtrate was evaporated to remove solvents at 50 °C. The product was dried under vacuum for 72 h at 60 °C.

Experimental set-up and procedure. The dead-end filtrations and enzymatic reaction were performed in a stirred cell (Amicon 8050, Millipore, USA) and descriptions of equipment and procedure can be found in previous work.⁸ The PLGC membranes (10 kDa) were placed on the membrane holder in ‘sandwich’ mode (with their own support layer facing the feed and an extra polypropylene support beneath the skin layer). The membrane was first soaked in a 5% NaCl solution for 30 min and then filtered with deionized water for another 30 min at 1 bar (procedures according to the manufacturers’ instructions). Next, the water permeability of the membranes was measured at 2 bar with buffer for 30 min. Then each enzyme solution (30 mL) was poured into the cell with a 10 kDa membrane for enzyme immobilization. The prepared solution was bubbled with CO₂ through a syringe needle (0.6 mm × 25 mm) before entering the reactor. The flow rate of gas (measured by the speed of bubble emission) was controlled in the same manner in all the experiments by controlling the pressure valve.

Solubility experimental apparatus and procedure. The gas solubility experimental apparatus and procedure are similar to the work of Shang et al. In the experiment CO₂ of ambient pressure was bubbled at a flow rate of about 60 mL min⁻¹ through about 4.0 g of the IL in a glass tube with an inner diameter of 12 mm. The glass tube was partly immersed in a water bath of desired temperature. The weight of the IL solution was determined at regular intervals by an electronic balance (OHAUS Corp. AR2140, USA) with a resolution of 0.0001 g.

Enzyme immobilization. Three enzymes of 100 mL liquid FDH, 1.0 mg solid FaldDH, and 1.5 mg solid ADH were immobilized in the 10 kDa regenerated cellulose membrane. Enzyme immobilization was carried out at a pressure of 2 bar, and permeate was collected in precision cylinders for analysis. The cylinders were replaced manually for every 4 mL. At the end of filtration, the ‘fouled’ membrane was washed with 10 mL of buffer at a pressure of 2 bar, and then rinsed 3 times with buffer without pressure. The amount of immobilized enzyme (loading) was calculated from the mass balance equation, and the immobilization efficiency was expressed as enzyme loading efficiency (loading efficiency = $\frac{m_i}{m_t}$) where m_i and m_t are amount of immobilized and total enzyme, respectively.

Enzymatic reaction with immobilized enzymes. NADH solution (5 mM) was prepared with 0.1 M Tris-HCl buffer and ILs which had been pre-bubbled with CO₂ for 30 min. 4 mL NADH solution with saturated CO₂ was added to the stirred cell equipped with 10 kDa regenerated cellulose membrane. The applied pressure was controlled manually to ensure that 4 mL permeate was obtained in 30 min. For the enzyme reuse experiment, when 4 mL of permeate had been obtained, the filtration was paused and another 4 mL of fresh NADH solution with saturated CO₂ was added for the next cycle (each cycle lasted about 30 min).

Enzymatic reaction with NADH regeneration. 2 mg of additional glucose dehydrogenase (GDH) for NADH regeneration was immobilized together with the other three enzymes (i.e. FDH, FaldDH, ADH) in the 10 kDa regenerated cellulose membrane. Immobilization procedure was the same as given above. The 4 mL NADH solution with saturated CO₂ containing 5 mM NADH and 50 mM D-Glucose as substrate for glucose dehydrogenase was run through the membrane. The obtained permeate was recycled as feed solution in the next reaction cycle and this operation was repeated for six times.

Analytical methods. The concentration of enzymes was measured as protein concentration using the Bradford protein assay (Perkin Elmer lambda20 UV/VIS, Germany). A Hewlett Packard HP6890 gas chromatograph (GC)

equipped with a FID (250 °C) and a Restek XTI-5 column (30 m × 0.25 mm i.d., film thickness 0.25 mm) was used for methanol concentration. The carrier gas was N₂ with a flow rate of 0.4 mL min⁻¹. The injector temperature was 150 °C and the injection volume was 1 mL. Methanol GC chromatograms were calibrated with 0.01–1 mM methanol solution in 0.1 M pH 7.0 Tris–HCl buffer. Scanning electron microscopy (SEM) was performed in an FEI Helios EBS3 dual beam electron microscope. The skin and support samples were prepared by cutting a small square of the membrane, which was then attached to an aluminium stub by means of double sided sticky carbon tape. The edges of the sample were mounted on the aluminium stub by means of copper tape. After freezing the membrane sample by plunging in liquid nitrogen, cross sections of the membrane skin and the support were cut from the with a pair of scissors. The cross sections were mounted on a slotted specimen stub and fixed with copper tape. All samples were coated with Pt for 2 s at 80 mA in a Cressington 208HR Sputter Coater, which gave an approximate thickness of 4 nm. The micrographs were obtained with an Everhart Thornley detector at low magnifications and with a Thru-the-Lens detector at high magnifications, in high vacuum at 5 keV acceleration voltage and 43 pA current. ¹H NMR measurements. Spectra were recorded at 298 K on a Varian XL-600 spectrometer operating at 600 MHz. Solutions were prepared by dissolving 20–30 mg of IL in 0.7 mL of D₂O.

Isothermal titration calorimetry. The titration experiments were performed using a Nano ITC low volume titration calorimeter (TA instruments, New Castle, DE, USA). Titrations were performed at 25 °C and consisted of enzyme (FDH) and 4.0 µL injections of ligand (NaHCO₃, sodium formate, NADH, or NAD⁺) at 300-second intervals. All solutions were filtered, degassed to avoid bubble formation, and equilibrated to the corresponding temperature before each experiment. The syringe was inserted into the reaction cell, stirring (250 rpm) was initiated, and the instrument was equilibrated at 25 °C until the base line was flat and stable. The titration data were analyzed with Nano Analyze software (TA Instruments) using an independent model to obtain the curve fitting and thermodynamic binding data. Enthalpy of binding was determined for three titrations of each experiment and average values were compared. The intrinsic molar enthalpy change (ΔH), the binding stoichiometry (n) and binding constant (K) for the binding process were obtained from the best fit of the calorimetric data. Gibbs free energy of binding and K_d were calculated from binding affinity measurements, using $\Delta G = -R(T) \ln(1/K_d)$, where R is the universal gas constant and T is temperature in Kelvin. Entropy of binding was then estimated with $\Delta S = (\Delta H - \Delta G) / T$, where ΔH was the average enthalpy of binding.

Molecular dynamic simulations. Molecular dynamics (MD) simulations were carried out to study the effect of the employed IL water mixtures on FDH. Therefore the structure of FDH from *Candida biodinii* (pdb code 5DN9) in complex with NAD⁺ and azide was downloaded from the PDB database. In preparation for the MD simulations the azide was replaced with a CO₂ molecule in both monomers of the enzyme using the *replace* function of YASARA 16.9.23 (YASARA Biosciences GmbH, Vienna, Austria).⁵⁰ Next, the program was used to clean the structure and optimize the hydrogen bonding network. To run the simulation in a mixed solvent system, a cubic simulation cell extending 10 Å around all atoms was created and the AMBER15IPQ force field was chosen.⁵¹ A cell neutralization and pK_a prediction experiment at pH 6.85 was carried out to neutralize the simulation cell and assign correct protonation states of the amino acid side-chains. For creation of the mixed solvent system, all water molecules were deleted from the soup and the solvent density was estimated using weighted densities of the pure compounds as found in the literature.⁵² The specific IL molecules were created using the *Build* function of YASARA to fill the simulation cell with an aqueous ionic liquid. In the next step the cell was filled with the created molecule using the respective densities specified in Table S3. The rest of the cell was filled with water molecules by temporarily removing the IL molecules, filling the cell with water using the specified density (Table S3), and adding the removed IL molecules back again. To remove all bumps between solvent molecules, the protein was fixed and an energy minimization experiment was carried out. Then all atoms were freed again and the resulting scene was saved as solvent system for the MD simulations. The simulations themselves were done using

the YASARA macro md_run with the pressure control mode “Manometer”, pH 6.85 and 298 K over a time of 18.1 ns. The resulting simulation snapshots were analysed using the YASARA macros md_analyze and md_analyzeres. For visualization in PyMOL (The PyMOL molecular Graphics System, Version 1.1 Schrodinger, Cambridge, MA, USA), the simulation file was converted to pdb using the YASARA macro md_convert. The movies were prepared using OBS Studio (<https://obsproject.com>)

References

1. Lim XZ. How to Make the Most of Carbon Dioxide. *Nature* **526**, 628–630 (2015).
2. Al-Saleh YM, Vidican G, Natarajan L, Theeyattuparampil VV. Carbon capture, utilisation and storage scenarios for the Gulf Cooperation Council region: A Delphi-based foresight study. *Futures* **44**, 105–115 (2012).
3. Xu XD, Moulijn JA. Mitigation of CO₂ by chemical conversion: Plausible chemical reactions and promising products. *Energ Fuel* **10**, 305–325 (1996).
4. Hou WB, Hung WH, Pavaskar P, Goepfert A, Aykol M, Cronin SB. Photocatalytic Conversion of CO₂ to Hydrocarbon Fuels via Plasmon-Enhanced Absorption and Metallic Interband Transitions. *Acs Catal* **1**, 929–936 (2011).
5. Li H, *et al.* Integrated Electromicrobial Conversion of CO₂ to Higher Alcohols. *Science* **335**, 1596–1596 (2012).
6. Shi JF, *et al.* Enzymatic conversion of carbon dioxide. *Chem Soc Rev* **44**, 5981–6000 (2015).
7. Obert R, Dave BC. Enzymatic conversion of carbon dioxide to methanol: Enhanced methanol production in silica sol-gel matrices. *J Am Chem Soc* **121**, 12192–12193 (1999).
8. Luo JQ, Meyer AS, Mateiu RV, Pinelo M. Cascade catalysis in membranes with enzyme immobilization for multi-enzymatic conversion of CO₂ to methanol. *New Biotechnol* **32**, 319–327 (2015).
9. Ulrich RUSCHING UM, Peter WILLNOW, Thomas HÖPNER. CO₂ Reduction to Formate by NADH Catalysed by Formate Dehydrogenase from Pseudomonas

oxalaticus. *European Journal of Biochemistry* **70**, 325–330 (1976).

10. Cui GK, Wang JJ, Zhang SJ. Active chemisorption sites in functionalized ionic liquids for carbon capture. *Chem Soc Rev* **45**, 4307–4339 (2016).
11. Bates ED, Mayton RD, Ntai I, Davis JH. CO₂ capture by a task-specific ionic liquid. *J Am Chem Soc* **124**, 926–927 (2002).
12. Gurkan BE, *et al.* Equimolar CO₂ Absorption by Anion-Functionalized Ionic Liquids. *J Am Chem Soc* **132**, 2116–+ (2010).
13. Rosen BA, Zhu W, Kaul G, Salehi-Khojin A, Masel RI. Water Enhancement of CO₂ Conversion on Silver in 1-Ethyl-3-Methylimidazolium Tetrafluoroborate. *J Electrochem Soc* **160**, H138–H141 (2013).
14. Whipple DT, Kenis PJA. Prospects of CO₂ Utilization via Direct Heterogeneous Electrochemical Reduction. *J Phys Chem Lett* **1**, 3451–3458 (2010).
15. Hussain W, Pollard DJ, Truppo M, Lye GJ. Enzymatic ketone reductions with co-factor recycling: Improved reactions with ionic liquid co-solvents. *J Mol Catal B-Enzym* **55**, 19–29 (2008).
16. Datta S, *et al.* Ionic liquid tolerant hyperthermophilic cellulases for biomass pretreatment and hydrolysis. *Green Chem* **12**, 338–345 (2010).
17. Eckstein M, Vilella M, Liese A, Kragl U. Use of an ionic liquid in a two-phase system to improve an alcohol dehydrogenase catalysed reduction. *Chem Commun*, 1084–1085 (2004).
18. Lau RM, van Rantwijk F, Seddon KR, Sheldon RA. Lipase-catalyzed reactions in ionic liquids. *Org Lett* **2**, 4189–4191 (2000).
19. Weaver KD, Kim HJ, Sun JZ, MacFarlane DR, Elliott GD. Cyto-toxicity and biocompatibility of a family of choline phosphate ionic liquids designed for pharmaceutical applications. *Green Chem* **12**, 507–513 (2010).
20. Fujita K MD, Forsyth M. Protein solubilising and stabilising ionic

liquids. *Chem Commun* **38**, 4804–4806 (2005).

21. Fujita K FM, MacFarlane DR, Reid RW, Elliott GD. Unexpected improvement in stability and utility of cytochrome c by solution in biocompatible ionic liquids. *Biotechnol Bioeng* **94**, 1209–1213 (2006).

22. Silva FAE, *et al.* Sustainable design for environment-friendly mono and dicationic cholinium-based ionic liquids. *Ecotox Environ Safe* **108**, 302–310 (2014).

23. Petkovic M, *et al.* Novel biocompatible cholinium-based ionic liquids–toxicity and biodegradability. *Green Chem* **12**, 643–649 (2010).

24. Luo JQ, *et al.* Directing filtration to optimize enzyme immobilization in reactive membranes. *J Membrane Sci* **459**, 1–11 (2014).

25. Wang XL, *et al.* Bioinspired Approach to Multienzyme Cascade System Construction for Efficient Carbon Dioxide Reduction. *Acs Catal* **4**, 962–972 (2014).

26. Marpani F, Sarossy Z, Pinelo M, Meyer AS. Kinetics based reaction optimization of enzyme catalyzed reduction of formaldehyde to methanol with synchronous cofactor regeneration. *Biotechnol Bioeng* **114**, 2762–2770 (2017).

27. Affandy A, Keshavarz-Moore E, Versteeg HK. Application of filtration blocking models to describe fouling and transmission of large plasmids DNA in sterile filtration. *J Membrane Sci* **437**, 150–159 (2013).

28. Palacio L, Ho CC, Zydney AL. Application of a pore-blockage – Cake-filtration model to protein fouling during microfiltration. *Biotechnol Bioeng* **79**, 260–270 (2002).

29. Li XY, *et al.* Absorption of CO₂ by ionic liquid/polyethylene glycol mixture and the thermodynamic parameters. *Green Chem* **10**, 879–884 (2008).

30. Jianmin Zhang SZ, Kun Dong, Yanqiang Zhang, Youqing Shen, Xingmei Lv. Supported Absorption of CO₂ by TetrabutylphosphoniumAmino Acid Ionic Liquids. *Chem-Eur J* **12**, 4021–4026 (2006).

- 507
508 31. Dean JA. *Lange's Handbook of Chemistry*.
509
510 32. Shengjuan Yuan YC, Xiaoyan Ji, Zhuhong Yang, Xiaohua Lu Experimental
511 study of CO₂ absorption in aqueous cholinium-based ionic liquids.
512 *Fluid Phase Equilib* **445**, 14–24 (2017).
513
514 33. Wang YZ, Li MF, Zhao ZP, Liu WF. Effect of carbonic anhydrase on
515 enzymatic conversion of CO₂ to formic acid and optimization of
516 reaction conditions. *J Mol Catal B-Enzym* **116**, 89–94 (2015).
517
518 34. Yuki Kohno HO. Ionic liquid/water mixtures: from hostility to
519 conciliation. *Chem Commun* **48**, 7119–7130 (2012).
520
521 35. Hermann Weingärtner CC, Christian Herrmann How ionic liquids can
522 help to stabilize native proteins. *Phys Chem Chem Phys* **14**, 415–426
523 (2012).
524
525 36. Marc L. Pusey MSP, Megan B. Turner, and Robin D. Rogers. Protein
526 crystallization using room temperature ionic liquids *Crystal Growth*
527 *& Design* **7**, 787–793 (2007).
528
529 37. Natalie Debeljuh CJB, Luke Hendersonb, Nolene Byrne. Structure
530 inducing ionic liquids—enhancement of alpha helicity in the
531 Abeta(1–40) peptide from Alzheimer's disease. *Chem Commun* **47**, 6371–
532 6373 (2011).
533
534 38. Megan B. Turner SKS, Jonathan G. Huddleston, John D. Holbreya, Robin
535 D. Rogers. Ionic liquid salt-induced inactivation and unfolding of
536 cellulase from *Trichoderma reesei*. *Green Chem* **5**, 443–447 (2003).
537
538 39. Seddon DSHAJSASR. Enzyme aggregation in ionic liquids studied by
539 dynamic light scattering and small angle neutron scattering. *Green*
540 *Chem* **9**, 859–867 (2007).
541
542 40. Liu WF, Hou YH, Hou BX, Zhao ZP. Enzyme-catalyzed Sequential
543 Reduction of Carbon Dioxide to Formaldehyde. *Chinese J Chem Eng* **22**,
544 1328–1332 (2014).
545
546 41. Sarcar S, Jain TK, Maitra A. Activity and Stability of Yeast
547 Alcohol-Dehydrogenase (Yadh) Entrapped in Aerosol Ot Reverse
548 Micelles. *Biotechnol Bioeng* **39**, 474–478 (1992).

549
550 42. Baskaya FS, Zhao XY, Flickinger MC, Wang P. Thermodynamic
551 Feasibility of Enzymatic Reduction of Carbon Dioxide to Methanol.
552 *Appl Biochem Biotech* **162**, 391-398 (2010).

553
554 43. Qianyun Sun YJ, Zhongyi Jiang, Lei Zhang, Xiaohui Sun, Jian Li.
555 Green and Efficient Conversion of CO₂ to Methanol by Biomimetic
556 Coimmobilization of Three Dehydrogenases in Protamine-Templated
557 Titania. *Ind Eng Chem Res* **48**, 4210-4215 (2009).

558
559 44. Bilal El-Zahab DD, Ping wang. Particle-tethered NADH for production
560 of methanol from CO₂ catalyzed by coimmobilized enzymes. *Biotechnol*
561 *Bioeng* **99**, 508-514 (2007).

562
563 45. Rémi Cazelles JD, François Fajula, Ovidiu Ersen, Simona Moldovanb,
564 Anne Galarneau. Reduction of CO₂ to methanol by a polyenzymatic
565 system encapsulated in phospholipids-silica nanocapsules. *New J*
566 *Chem* **37**, 3721-3730 (2013).

567
568 46. Xiaoyuan Ji ZS, Ping Wang, Guanghui Ma, Songping Zhang. Tethering of
569 Nicotinamide Adenine Dinucleotide Inside Hollow Nanofibers for High-
570 Yield Synthesis of Methanol from Carbon Dioxide Catalyzed by
571 Coencapsulated Multienzymes. *Acs Nano* **9**, 4600-4610 (2015).

572
573 47. Obón JM MA, Iborra JL. Retention and regeneration of native NAD(H)
574 in noncharged ultrafiltration membrane reactors: application to L-
575 lactate and gluconate production. *Biotechnol Bioeng* **57**, 510-517
576 (1998).

577
578 48. R. Castillo MO, S. Martí, V. Moliner. A Theoretical Study of the
579 Catalytic Mechanism of Formate Dehydrogenase. *J Phys Chem B* **32**,
580 10012-10022 (2008).

581
582 49. De Santis S, *et al.* Cholinium-amino acid based ionic liquids: a new
583 method of synthesis and physico-chemical characterization. *Phys Chem*
584 *Chem Phys* **17**, 20687-20698 (2015).

585
586 50. Krieger E, Vriend G. YASARA View-molecular graphics for all devices-
587 from smartphones to workstations. *Bioinformatics* **30**, 2981-2982
588 (2014).

589
590 51. Debiec KT, Cerutti DS, Baker LR, Gronenborn AM, Case DA, Chong LT.
591 Further along the Road Less Traveled: AMBER ff15ipq, an Original

592 Protein Force Field Built on a Self-Consistent Physical Model. *J*
593 *Chem Theory Comput* **12**, 3926–3947 (2016).

594

595 52. del Olmo L, Lage-Estebanez I, Lopez R, de la Vega JMG. Understanding
596 the Structure and Properties of Cholinium Amino Acid Based Ionic
597 Liquids. *J Phys Chem B* **120**, 10327–10335 (2016).

598

599